Investigation of zinc borate-reinforced epoxy composites produced via additive manufacturing: thermal and mechanical analysis

Saadet Guler and Berk Ozler
Department of Metallurgical and Materials Engineering, Izmir Katip Celebi University, Izmir, Turkey
Ahmet Cagri Kilinc
Department of Mechanical Engineering, Osmaniye Korkut Ata University, Osmaniye, Turkey, and
Turker Turkoglu
Department of Mechanical Engineering, Balikesir University, Balikesir, Turkey

Abstract

Purpose – The purpose of this study is to investigate the production and performance of zinc borate–reinforced epoxy composites produced via additive manufacturing. This study aims to evaluate the effects of different zinc borate reinforcement ratios on the mechanical, thermal and fire retardancy properties of the composites. By analyzing the results, this study seeks to provide a deeper understanding of the potential of zinc borate as an eco-friendly flame retardant in advanced polymer composite applications.

Design/methodology/approach – Epoxy composites were reinforced with zinc borate at weight fractions of 0.5%, 1%, 2% and 3% using the stereolithography additive manufacturing method. The mechanical properties were characterized through tensile, three-point bending and dynamic mechanical analysis. Thermal properties were assessed using thermogravimetric analysis, and flame retardancy was evaluated with specific fire retardancy tests. Microstructural and chemical properties were examined via scanning electron microscopy, X-ray diffraction and Fourier-transform infrared spectroscopy analyses. In addition, hardness and thermal conductivity tests were performed to provide a comprehensive evaluation of the composites.

Findings – The incorporation of zinc borate significantly improved the thermal stability and mechanical properties of epoxy composites. Zinc borate acted as an effective flame retardant due to its hydrate groups, which enhanced thermal stability. However, the flame retardancy performance was found to be insufficient at lower reinforcement rates. This study highlights the potential of zinc borate as a multifunctional additive for enhancing the durability and performance of epoxy composites while emphasizing the need for further optimization to achieve superior flame retardancy.

Originality/value – This study represents an innovative approach by combining eco-friendly zinc borate reinforcement with advanced additive manufacturing techniques to produce high-performance polymer composites. It provides valuable insights into the interplay between reinforcement ratios and composite properties, offering a pathway for the optimization of zinc borate–reinforced materials. The findings contribute to the growing field of sustainable material development and establish a foundation for future studies in flame-retardant polymer composites.

Keywords Additive manufacturing, Zinc borate, Thermal stability, Mechanical properties, Composite

Paper type Research paper

1. Introduction

The increasing demand for high-performance polymer composites in industries such as aerospace, automotive and electronics has led to a heightened focus on fire safety and mechanical durability (Muhammad *et al.*, 2020; Tuli *et al.*, 2024). While polymers offer numerous advantages, including flexibility, low cost and ease of processing, their high flammability limits their applications in fire-prone environments (Guler *et al.*, 2025; Gupta *et al.*, 2024). The incorporation of flame-retardant additives becomes essential in polymer composites designed for use in environments where enhanced fire resistance is required. Among the environmentally friendly and effective flame retardants, zinc borate (ZB) has gained prominence due to its ability to reduce flammability, improve thermal stability and act synergistically with other fillers (Cuthbertson *et al.*, 2024; Dogan *et al.*, 2021; Lv *et al.*, 2020).

ZB is widely recognized as a multifunctional additive, used primarily for its flame-retardant properties in polymer matrices (Lu *et al.*, 2019; Zhou *et al.*, 2024a, 2024b). Its ability to

The current issue and full text archive of this journal is available on Emerald Insight at: **https://www.emerald.com/insight/1355-2546.htm**

Rapid Prototyping Journal
32/2 (2026) 434–445

[DOI 10.1108/RPJ-12-2024-0530]

Competing interests: The authors declare that they have no known competing financial interests or personal relationships that could have appeared to influence the work reported in this paper.

Received 30 December 2024
Revised 8 April 2025
30 July 2025
Accepted 8 September 2025

suppress flames, reduce smoke generation and improve char formation positions as a vital component in enhancing the fire safety of polymer composites. Moreover, ZB not only influences flame-retardant behavior but also enhances the mechanical and thermal performance of these materials, making it a versatile reinforcement (Chan-Hom *et al.*, 2017).

Recent advancements in additive manufacturing (AM) technologies, particularly stereolithography (SLA), have expanded the possibilities for fabricating complex polymeric structures with tailored properties (Sano *et al.*, 2018; Zhou *et al.*, 2024a, 2024b). SLA, a vat-photopolymerization technique, is valued for its high resolution and precise control over material composition, making it ideal for integrating flame retardants like ZB into polymer matrices. The layer-by-layer approach ensures a homogeneous distribution of ZB, enhancing the mechanical and thermal properties of the final product. In addition to improved material efficiency, SLA offers the flexibility to incorporate multiple materials and fillers, producing composites with superior properties. This makes it particularly useful for creating high-performance, flame-retardant materials in industries such as aerospace, automotive and electronics (Garcia *et al.*, 2024; Lodha *et al.*, 2023; Shen *et al.*, 2008).

In the literature on flame retardant materials, various manufacturing methods and additives have been used to enhance the fire resistance of polymer composites. In the study conducted by Lv *et al.* (2022), the flame-retardant properties of ULTEM 9085 polymer composites produced using the Fused Deposition Modeling method were investigated. The effects of infill density, sample thickness and the number of solid layers on both sides on flame length and heat release rate were examined. It was found that the highest flame length, approximately 80 mm, was recorded in samples with a 30% infill density. Yücesoy *et al.* (2023) aimed to enhance the flame-retardant efficiency and thermal stability of low-density polyethylene composites using halogen-free inorganic additives. In their study, various ratios of magnesium hydroxide and magnesium carbonate were used, and the addition of ZB resulted in a significant delay of 51.8°C in the thermal degradation temperature. Ozcelik *et al.* (2022) observed that boron compounds in thermoplastic polyurethane matrices exhibited superior flame-retardant performance compared to conventional mineral fillers. These findings highlight the synergistic effects of boron compounds and their potential to improve flame-retardant properties across different polymer matrices. This study advances existing research by incorporating ZB as a flame retardant into polymer composites produced via SLA, an advanced AM technique. Unlike traditional methods, SLA offers a novel approach for achieving homogeneous distribution of the flame retardant while enabling the creation of complex geometries with high precision. By examining varying reinforcement ratios and their impact on mechanical, thermal and flame-retardant properties, this work provides a unique contribution to the field of AM for high-performance materials.

In this study, the development of ZB-reinforced polymer composites using SLA was investigated, with reinforcement ratios of ZB set at 0.5%, 1%, 2% and 3%. The aim was to explore how these varying ratios affect the mechanical, thermal and flame-retardant properties of the composites. The mechanical properties were assessed through dynamic mechanical analysis, tensile and three-point bending tests, while thermal stability was evaluated using thermogravimetric analysis (TGA). In addition, the flame retardancy of the composites was tested to determine their effectiveness in fire scenarios. To provide a comprehensive analysis, the study also includes detailed surface morphology examinations using scanning electron microscopy (SEM) and chemical characterization through Fourier-transform infrared spectroscopy (FTIR). Hardness testing was conducted to evaluate the material's resistance to deformation and thermal conductivity tests were performed to assess the heat dissipation capabilities of the ZB-reinforced composites. The results from these tests will offer valuable insights into optimizing ZB loadings for achieving superior fire-resistant polymer composites.

2. Materials and methods

2.1 Materials

In the production of composite materials, epoxy-based photosensitive UV resin (AnyCubic UV Sensitive Resin) was used as the matrix material, while ZB particles (commercial ZB, REFSAN Co., Turkey; average particle size: 20.4 μm) were used as the reinforcement material. The components were combined and blended using mechanical and ultrasonic mixers. The resulting homogeneous composite resins were printed in three dimensions using a Creality Halot One CL-60 SLA-based LCD printer. The layer thickness, which is one of the printing parameters, was set at 100 μm, and the exposure time was set at 4 s. The abbreviations of the obtained ZB-reinforced composites, determined according to their contents, are shown in Table 1.

2.2 Characterization

Morphological and structural examinations of the materials were conducted using a scanning electron microscope (SEM). Images of the particles coated with Au-Pd were obtained with an accelerating voltage of 3 kV. Particle size distribution analysis of ZB particles was performed with dynamic light scattering (Zetasizer Nano ZS, Malvern Instruments). Phase structures of the particles were determined using an X-ray diffraction (XRD, Bruker D2 Phaser). In the scanning performed at a scanning speed of 5°/min in the range of $5^\circ \leq 2\theta \leq 90^\circ$, Cu-$K_\alpha$ radiation (1.5406 Å) was used. The search-matching process was conducted on the obtained spectra using HighScore software. Similarly, the organic bond structures of all samples were determined through FTIR. During the examination, Attenuated Total Reflectance equipment was used, with the wave number range set at 650–4,000 cm^{-1}. For each sample, 24 scans were performed.

2.3 Thermal properties

The thermal properties of the composite materials were determined through a series of analyses, including TGA, thermal

Table 1 Abbreviations of ZB-reinforced composites

Sample	Content weight percent (Wt %) Resin	ZB
Pristine	100	–
ZB1	99.5	0.5
ZB2	99	1
ZB3	98	2
ZB4	97	3

Source(s): Created by the authors

conductivity analysis and a flammability test. The degradation temperatures of the samples were determined by means of TGA (PerkinElmer STA8000). Each sample was subjected to a heating process, reaching a temperature of 800°C at a rate of 10°C per minute, in an inert nitrogen (N_2) atmosphere. Thermal conductivity measurements were obtained through thermal conductivity analysis (C-Therm TCi). Flame retardancy tests were conducted using a needle flame tester (Zhilitong ZLT-ZY2) in accordance with the Underwriters Laboratories 94 (UL94) standard (Spieß *et al.*, 2021).

2.4 Mechanical properties

The mechanical properties of the composites were determined through a series of tests, including tensile, three-point bending, hardness and dynamic mechanical analysis. Tensile and three-point bending tests (Shimadzu AG-50kNG) were conducted in accordance with the ASTM D638 (Peloquin *et al.*, 2023) and ASTM D790 standards (Tavangarian *et al.*, 2024), respectively, with a jaw speed of 1 mm/min. In the bending test, cylindrical supports were used as openings with a span-to-depth ratio of 16:1. The Shore D hardness device was used to ascertain the hardness values. Dynamic mechanical analysis (TA Instruments, Q800) tests of the composites were carried out to investigate their thermomechanical behavior, storage and loss modulus. Printed samples with dimensions of 35 × 10 × 3 mm were tested in bending mode at a frequency of 1 Hz by heating from room temperature to 140°C at a rate of 2°C/min.

3. Results and discussion

3.1 Morphological and structural analysis

SEM image of ZB particle is shown in Figure 1(a). As seen from the figure, most of the particles are in the form of clusters which have irregular geometry with variation in particle size. Higher magnification revealed that the particles are in the form of clusters composed of smaller particles with round edges. Particle size distribution (PSD) curve of ZB powder is shown in Figure 1(b), which conforms to bimodal Gaussian distribution. The particle sizes up to 4.06 μm represents 10% and the particle size up to 10.3 μm represents 50% and 20.4 μm represents 90% of particle size distribution.

XRD examination shown in Figure 1(c) shows that ZB hydrate and boron zinc phases exist in the crystal structure. The pronounced peaks in the graph indicate that these materials possess a highly crystalline structure. The distinctive peaks within the 2θ range denote the crystal phases of ZB hydrate, consistent with worldwide standard databases. The distinct phases of boron zinc were unequivocally recognized. In the XRD analysis, Boron Zinc (ZnB_4O_7) peaks corresponding to the main phase were observed at 21.3°, 27.5°, 30.7° and 37.9°. ZB hydrate ($4ZnO\text{-}B_2O_3\text{-}H_2O$) peaks were observed at 22.8°, 28.9°, 31.4° and 40.6°. The pronounced peak distribution, particularly between 20° and 50°, reinforces the structural stability and thermal characteristics of ZB. ZB is frequently used as a fire retardant, a characteristic attributed to the stability of its crystalline phases. Moreover, literature indicates that the material maintains its usefulness throughout dehydration in sintering due to its hydrate structure (Mahajan *et al.*, 2020). This XRD investigation validates the crystal structures of ZB and boron zinc, highlighting the significance of these materials in ceramics, fire retardants and various industrial uses. The phase study of these materials is essential for establishing process parameters and assessing application potential.

Figure 1(d) illustrates the TGA curve of ZB particles. In this analysis, the temperature increased from room temperature to 800°C and the weight loss percentages of ZB particles as a function of temperature were plotted. Upon examination of the figure, two distinct weight loss curves are observed. The curve between 70°C and 170°C indicates the removal of the moisture layer on the particle, while the curve between 350°C and 500°C indicates the removal of the crystal water (hydrate groups) within the particle structure.

SEM images of the fracture surfaces of composites containing between 0.5 Wt.% and 3 Wt.% ZB particles are shown in Figure 2(a)–(d). Upon examination of the figures, it is evident that the distribution of AB particles within the structure is homogeneous, and no voids or pores are observed, likely due to the effectiveness of the mixing process applied during production. Notably, while a smooth and even fracture surface is observed at low reinforcement levels, increasing the reinforcement amount results in greater roughness on the fracture surfaces. While the additive is in the form of agglomerated clusters with the increasing reinforcement amount, the fracture surface of composites changed from a smooth topography to a high-roughness surface with the increasing reinforcement amount. The reason for the change in the fracture surface depending on the increasing reinforcement amount can be explained by the act of particles as an obstacle to fracture propagation during the test (Perin *et al.*, 2023). However, when the reinforcement content exceeds 0.50 Wt.%, the agglomeration of particles was observed (Mubarak *et al.*, 2020) indicated that agglomeration may affect curing and cross-linking, causing a decrease in the mechanical properties of the composite which is in accordance with the mechanical properties (see Figure 8). In addition, partial fibrillation was observed with increasing reinforcement of ZB particles.

As seen in Table 2, the mean particle size and standard deviation values increased by increasing ZB content into the photocurable polymer resin. Increase in the mean particle size was attributed to the agglomeration of particles with increasing reinforcement content. Cross-sectional SEM images of composites (see Figure 3) revealed an increase in the particle size and higher magnification images of particles demonstrated the agglomeration.

3.2 Organic bond structures

The absorbance FTIR spectrums of pristine resin (as cured) and the composites containing various amounts of ZB between 0.5 Wt.% and 3 Wt.% are shown in Figure 4. The peaks located at 2,940 and 2,867 cm^{-1} are associated with the stretching vibration of $–CH_3$ and $–CH_2$ of resin respectively (Shan *et al.*, 2020). The sharp peak located at 1,726 cm^{-1} is associated with the stretching vibration of C = O found within the matrix 3. The peak located at 1,650 cm^{-1} corresponds to H-O-H bending vibration which is a characteristic peak for ZB heptahydrate (Durrani *et al.*, 2020). The peak located at 1450 cm^{-1} corresponds to the symmetric stretching of the C-H bonds within the CH_3 groups and this peak is also associated with the in-plane bending of B-O-H (Guler *et al.*, 2025; Tan *et al.*, 2020).

Figure 1 (a) SEM images at 2 and 10K magnification, (b) PSD curve depending on volume density, (c) XRD spectrum and (d) thermogravimetric analysis (TGA) of ZB particles

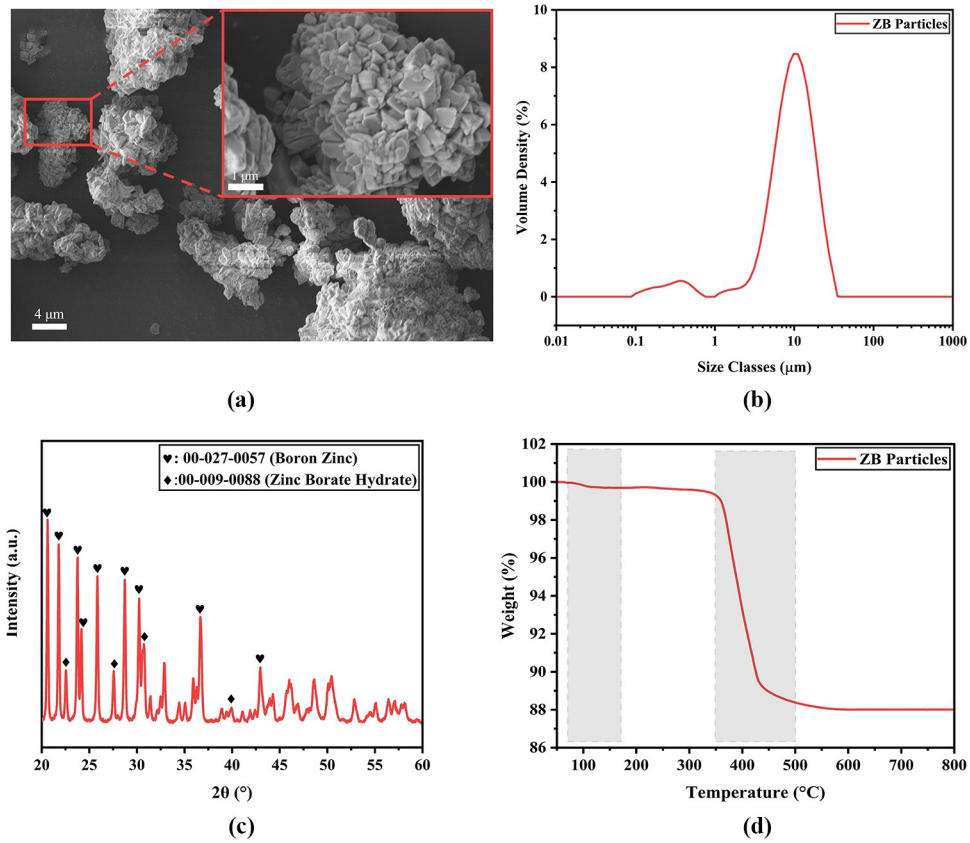

Source: Created by the authors

The peaks located at 1,410 and 1,339 cm^{-1} are assigned to asymmetric stretching vibrations of trihedral (BO_3) borate groups (Tan *et al.*, 2020; Tugrul *et al.*, 2015). The peaks located between 1,000–1,150 and 800–900 cm^{-1} which are overlapped with stretching vibration of the C-O and alkoxy C-O bond are also assigned to asymmetric and symmetric stretching vibrations of tetrahedral (BO_4) borate groups (Tugrul *et al.*, 2015). Absorbance intensities of these peaks were increased and became more distinctive with incorporation of ZB particles into resin matrix.

3.3 Thermal properties

TGA results shown in Figure 5 show the weight loss and thermal degradation behavior of pristine and ZB-reinforced composites (ZB1, ZB2, ZB3 and ZB4) with increasing temperature (from room temperature to 800°C). This analysis provides insights into the thermal stability and degradation characteristics of the samples, revealing the effect of ZB additive on thermal performance.

Figure 5(a) shows the TGA curves over a wide temperature range (from room temperature to 800°C). In the examined graph, no significant weight loss is observed up to 300°C. This situation shows that the material maintains its thermal stability up to a certain temperature. It is observed that a significant weight loss occurs between 350 and 500°C. This sudden decrease occurs as a result of the organic components in the composite matrix burning and leaving the structure. After 500°C, it is observed that the pristine sample experiences higher weight loss compared to those with ZB-reinforced. This situation indicates that the ZB additive remains in the structure up to 800°C.

Figure 5(b) focuses on the critical decomposition temperature range (300°C–550°C) for a more detailed examination. It can be seen more clearly in this graph that the composites with ZB additives exhibit a slight increase in the residual weight compared to the pristine sample. It can also be assumed that the ZB acts as a stabilizing agent, reducing the decomposition rate (reducing the slope of the curve) and thus increasing the overall thermal resistance of the material.

The results of TGA show that the inclusion of ZB increases the thermal stability of epoxy-based composites. This improvement can be evidenced by the slowing down of the degradation rate of the organic structure. The observed thermal stabilization effect can be attributed to the inherent flame-retardant properties of ZB, which acts as a thermal barrier during decomposition. This behavior can be explained by the endothermic decomposition of the material, which absorbs heat while diluting the flammable volatiles produced during matrix degradation and releasing non-flammable gases (Raslan *et al.*, 2019). This mechanism has been confirmed by previous studies showing that ZB increases both the thermal and flame-retardant properties of polymer composites (Mahajan *et al.*, 2020;

Figure 2 SEM images of fracture surfaces of ZB-reinforced composites at different reinforcement ratios

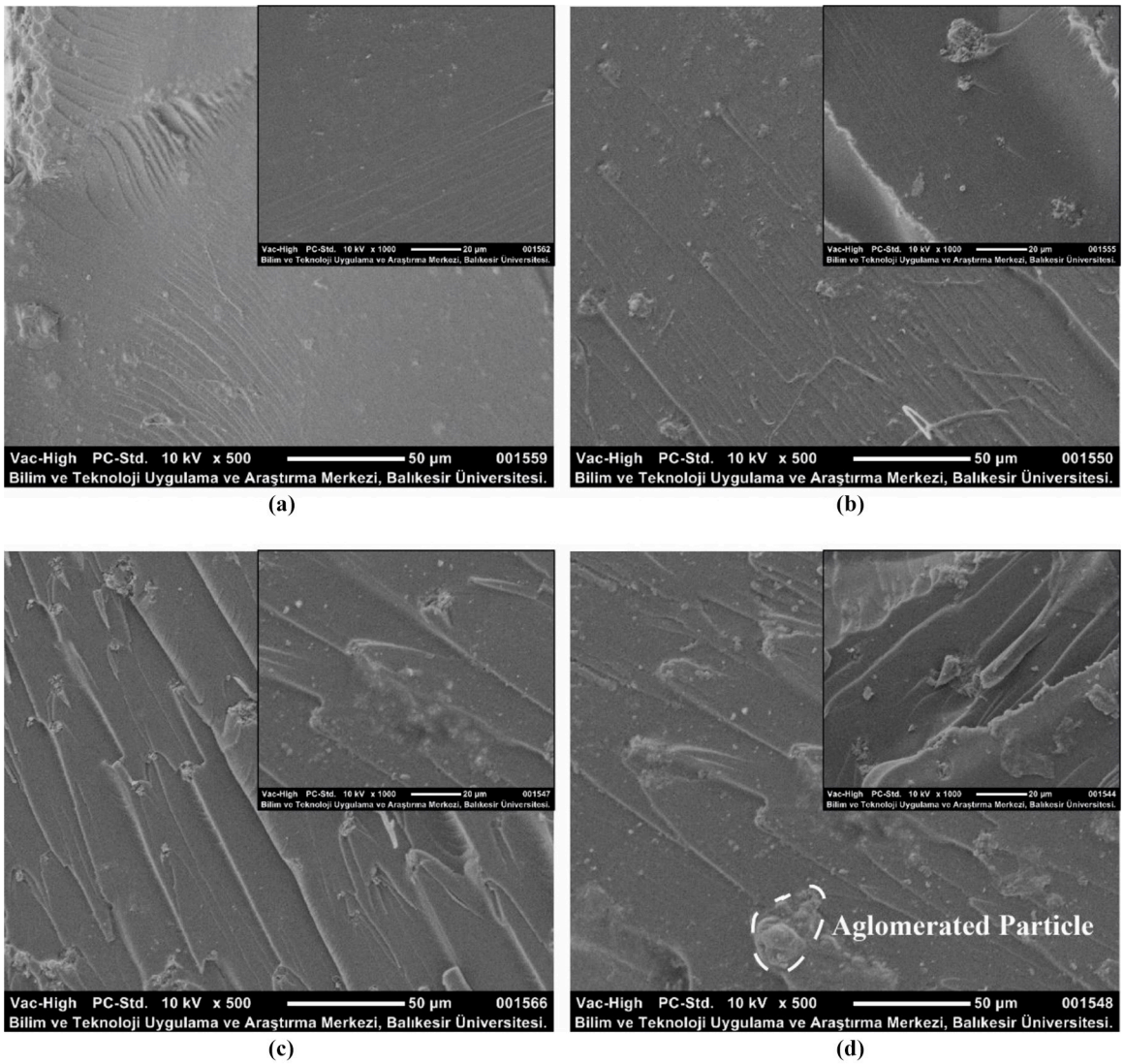

Note(s): (a) 0.5 Wt.% (ZB1), (b) 1 Wt.% (ZB2), (c) 2 Wt.% (ZB3) and (d) 3 Wt.% (ZB4)
Source: Created by the authors

Table 2 Mean particle size values measured based on the cross-sectional SEM images of composites

Sample	Mean particle size (μm)
ZB2	21.53 ± 11.93
ZB3	28.87 ± 15.73
ZB4	35.36 ± 20.48

Source(s): Created by the authors

Raslan *et al.*, 2019). The data also show that there is a direct relationship between ZB content and thermal stability, and that higher concentrations can result in more significant improvements.

Figure 6 shows the thermal conductivity values of pristine and ZB-reinforced epoxy composites. While ZB reinforcement is seen to increase the thermal conductivity in general, there is also a fluctuation in the thermal conductivity values with changing ZB concentrations (ZB1, ZB2, ZB3 and ZB4). This trend indicates that the distribution of the ZB filler in the epoxy matrix creates a complex interaction and causes fluctuation by forming agglomeration.

When ZB particles are optimally distributed within the composite structure, they facilitate phonon conduction and thus increase the overall thermal conductivity of the composite. However, as the particle amount increases, they can agglomerate and disrupt the conductive network formed within the matrix, creating local thermal barriers (Burger *et al.*, 2016). The increase in thermal conductivity observed in ZB1 and ZB3 samples and the decrease observed in ZB2 and ZB4 samples can be expressed with this situation. These findings indicate that ZB can increase thermal conductivity in epoxy composites if the optimum concentration and homogeneous distribution are provided (Canıtez *et al.*, 2023). Therefore, it is essential to provide these conditions to benefit from the thermal

Figure 3 SEM images of agglomerated particles

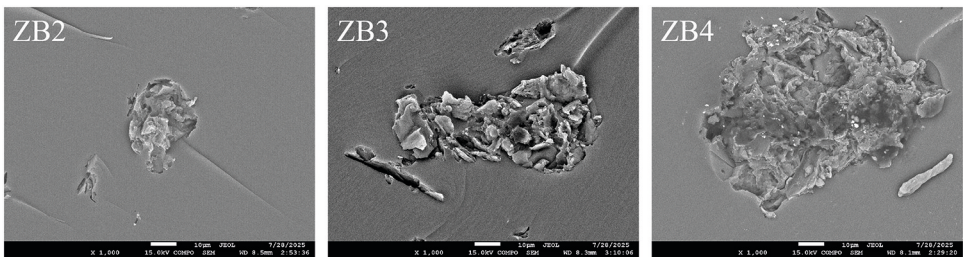

Source: Created by the authors

Figure 4 FT-IR spectrum of pristine and ZB-reinforced composites

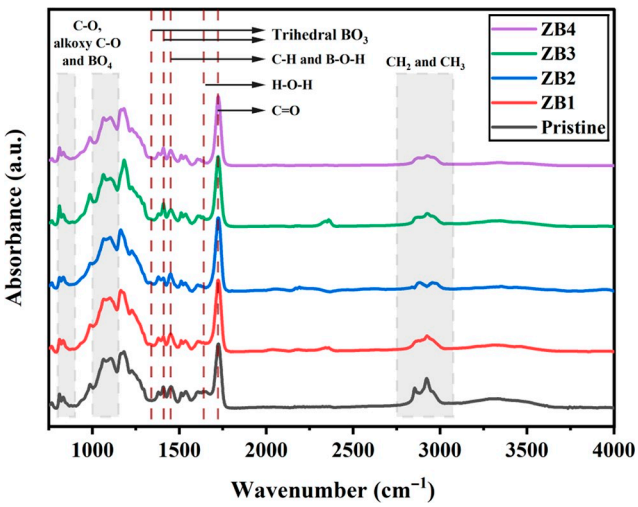

Source: Created by the authors

conductivity benefits of ZB in polymer-based applications requiring improved thermal management.

For the flame retardancy test, samples with dimensions of 125x13x3 mm were printed from Pristine and ZB-reinforced composite (0.5%, 1%, 2% and 3% by weight) resins in UL94 standard. As a result of the test, all samples were observed to ignite and burn in the first 10 s. No melting (dripping) occurred on the samples; however, it was determined that the samples continued to burn in the 30-s period after they were removed from the flame. When Figure 7(a)–(e) was examined, no significant difference was observed in carbonization, burn marks and general surface residues between the samples despite the increase in the additive rates. When the Pristine sample and the 3% ZB-reinforced sample were compared, it was observed that the density and distribution properties of the carbon layers formed after combustion were similar.

As a result, it shows that the flame-retardant effect of ZB is insufficient at the studied rates and does not provide an improvement with the increasing additive amount. This situation is contrary to the literature (Gillani *et al.*, 2018; Yildiz *et al.*, 2009) and suggests that the ZB additive may not be homogeneously distributed in the polymer matrix and therefore the ZB reinforcement on the sample surface is not sufficient. For future studies, the use of ZB additive in different polymer matrix materials, its combination with other flame-retardant additives or modifications to increase the ZB additive ratio are recommended.

3.4 Mechanical properties

The tensile strength values for ZB-reinforced polymer composites with varying reinforcement ratios, produced using SLA are presented in Figure 8. The results indicate that the tensile strength of the composites changes depending on the amount of ZB added to the polymer matrix, with each

Figure 5 TGA results of pristine and ZB-reinforced composites (ZB1, ZB2, ZB3 and ZB4 for 0.5, 1, 2 and 3 Wt.%, respectively.) with (a) wide temperature range and (b) critical decomposition temperature range

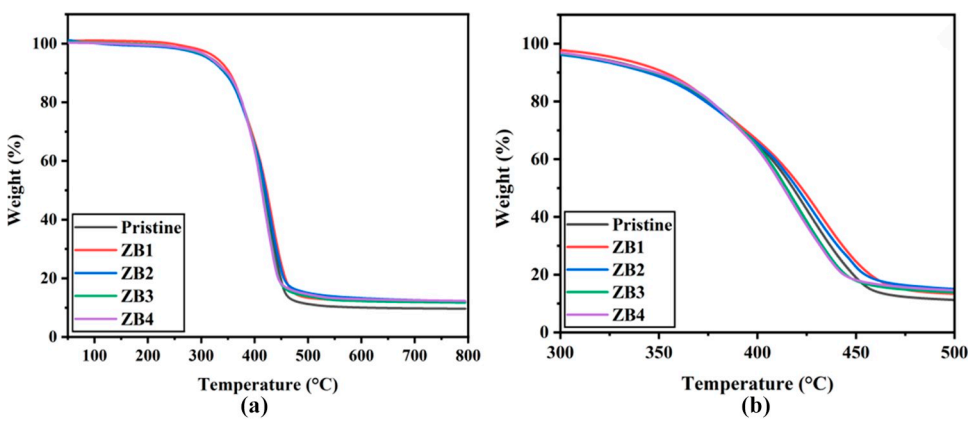

Source: Created by the authors

Figure 6 Thermal conductivity of pristine and ZB-reinforced composites

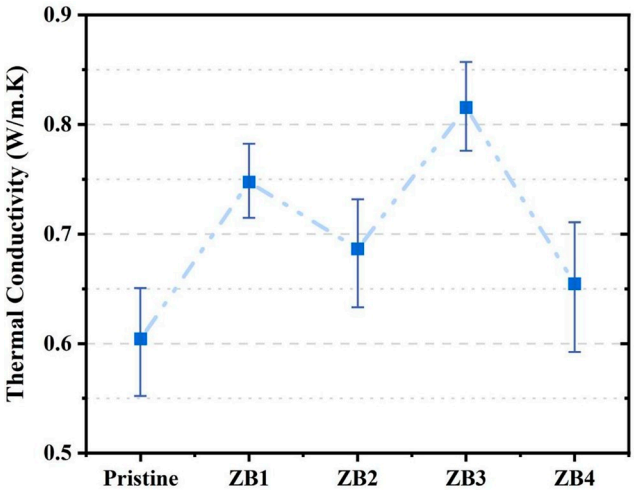

Source: Created by the authors

reinforcement level showing substantial effects on mechanical performance.

For the composite with 0.5 Wt.% ZB reinforcement, the average tensile strength was measured as 47.89 MPa, showing a notable improvement compared to the unreinforced matrix, which exhibited a tensile strength of 36.44 MPa. This increase of approximately 31.4% suggests that a small amount of ZB reinforcement can significantly enhance the composite's tensile properties by improving load distribution within the matrix. The use of SLA technology in fabricating these composites allows for a precise distribution of the ZB particles, contributing to a uniform load transfer across the material. In the case of the 1 Wt.% ZB composite, the tensile strength values were recorded as 48.08 and 41.52 MPa, with an average of 44.80 MPa. This reinforcement level initially resulted in improved tensile strength, with the maximum value observed at 48.08 MPa; however, the lower value indicates some variability, potentially due to minor agglomeration of ZB particles. Such agglomeration may act as stress concentrators, reducing the uniformity of load distribution and partially offsetting the reinforcement effect. SLA's layer-by-layer fabrication process aids in achieving homogeneity, yet particle

Figure 8 Stress-strain curve of pristine and ZB-reinforced composites after tensile test

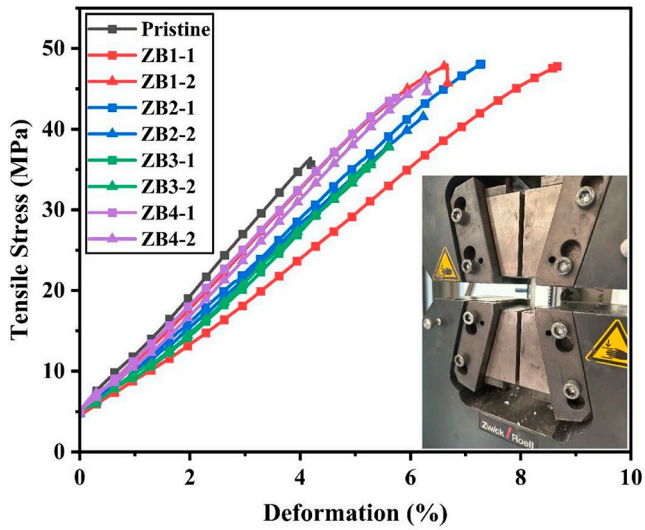

Source: Created by the authors

compatibility and dispersion within the polymer matrix remain essential factors in achieving optimal mechanical performance. For the composite reinforced with 2 Wt.% ZB, the tensile strength values decreased to 35.69 MPa and 37.79 MPa, averaging 36.74 MPa, which is comparable to the unreinforced matrix. This result suggests that at higher reinforcement levels, the compatibility between ZB particles and the polymer matrix may diminish, leading to particle agglomeration. The agglomerates may create stress points that hinder load transfer within the matrix, resulting in a decrease in tensile strength, despite the precise control offered by SLA. The composite with 3 Wt.% ZB displayed tensile strengths of 44.21 MPa and 46.17 MPa, with an average of 45.19 MPa. Although these values are higher than those of the unreinforced matrix, they are lower than the optimal results observed at 0.5 Wt.%. This suggests that while higher ZB content can provide reinforcement, excessive amounts may lead to diminishing returns due to particle agglomeration, which reduces effective load transfer and may restrict polymer chain mobility within the matrix. Even with SLA's capacity for high precision, excessive filler

Figure 7 Images of (a) pristine, (b) ZB1, (c) ZB2, (d) ZB3 and (e) ZB4 composite samples taken after the flammability test

Source: Created by the authors

amounts can create heterogeneity in the material structure. Finally, these findings indicate that an optimal ZB concentration exists for maximizing tensile strength in SLA-produced polymer composites. The results suggest that 0.5 Wt.% ZB provides the most effective reinforcement, enhancing tensile strength by promoting uniform load distribution and benefiting from the precise layer-by-layer control of the SLA process. At higher reinforcement levels, particle agglomeration likely counteracts the reinforcement effect, aligning with previous studies that report similar trends in particle-reinforced composites produced via AM.

When fillers are introduced, they occupy the spaces between polymer chains, leading to a reduction in free volume and facilitating closer packing of the polymer molecules. This closer packing enhances the load transfer mechanism within the material, reducing localized deformation and maintaining the structural integrity of the polymer (Pinto *et al.*, 2001; Russo *et al.*, 2013). The decrease in tensile strength observed at higher ZB concentrations may be attributed to the impact of additives on the alignment and entanglement of polymer chains within the matrix. High levels of additives can disrupt the orderly arrangement of polymer chains, leading to a reduction in tensile strength. In particular, agglomeration at elevated additive concentrations may hinder effective load transfer, thus limiting the material's mechanical performance. This phenomenon is also supported by findings from (Desai *et al.*, 2024), who reported similar effects of additive-induced agglomeration on mechanical properties in polymer composites. In addition, the slight increase in hardness at specific ZB levels can be explained by the enhanced packing density of the polymer matrix, resulting in improved compaction properties within the structure.

The three-point bending test results for the ZB-reinforced polymer composites with varying reinforcement amounts are presented in Table 1. The results demonstrate that the average bending strength values vary depending on the amount of ZB added. The composites with 0.5 Wt.% of ZB (ZB1) exhibited an average bending strength of 69.46 MPa, while the composites with 1.0 Wt.% (ZB2), 2.0 Wt.% (ZB3) and 3.0 Wt.% (ZB4) of ZB displayed average bending strengths of 63.27 MPa, 65.55 MPa and 63.69 MPa, respectively.

As shown in Figure 9(a)–(d), the bending test results for composites with different ZB reinforcement ratios are illustrated. The dashed red line in the figure represents the bending strength of the unreinforced matrix, which is 50 MPa. The current bending strength values for each composite are compared to this reference point, providing a clear indication of the improvement achieved through ZB reinforcement.

The composite with 0.5 Wt.% ZB (ZB1) demonstrated the highest bending strength of 69.46 MPa, representing a 39.0% increase compared to the unreinforced matrix. This substantial improvement suggests that a small amount of ZB reinforcement effectively enhances the mechanical properties of the composite. Similarly, the composite with 1.0 Wt.% ZB (ZB2) exhibited a bending strength of 63.27 MPa, which corresponds to a 26.5% increase over the unreinforced matrix. Despite the increase in reinforcement, this sample showed a lower bending strength compared to the ZB1 sample, indicating that an optimal reinforcement level may exist.

Further analysis shows that the composite with 2.0 Wt.% ZB (ZB3) achieved a bending strength of 65.55 MPa, resulting in a 31.1% increase compared to the matrix without reinforcement. Although this is an improvement over the unreinforced matrix, it is lower than the bending strength of the ZB1 sample, suggesting that increasing the ZB content beyond 0.5 Wt.% may not necessarily yield a proportional increase in mechanical performance.

Finally, the composite with 3.0 Wt.% ZB (ZB4) exhibited a bending strength of 63.69 MPa, indicating a 27.4% increase over the unreinforced matrix. However, similar to the ZB2 sample, the bending strength decreased as the ZB content increased beyond a certain threshold. This reduction in performance could be attributed to the agglomeration of ZB particles at higher concentrations, which may act as stress concentrators, thereby negatively affecting the composite's load-bearing capacity.

In conclusion, the results indicate that ZB reinforcement improves the bending strength of polymer composites, with the highest performance achieved at a reinforcement level of 0.5 Wt.%. Beyond this point, the mechanical properties show diminishing returns, likely due to particle agglomeration. These findings suggest that there is an optimal ZB concentration that balances mechanical performance and flame retardancy, aligning with previous research on particle-reinforced composites. The addition of boron-containing additives in high amounts causes the deterioration of mechanical properties in polymers, as also noted by (Dogan *et al.*, 2021) in their study on boron-based flame retardants. The observed deterioration in mechanical properties can be attributed to the incompatibility between the additives and the polymer matrix, leading to the formation of agglomerated particles and stress centers, which limit the mobility of polymer chains. This is consistent with the findings of (Yücesoy *et al.*, 2023), who reported similar effects in low-density polyethylene composites reinforced with magnesium hydroxide and magnesium carbonate at high additive content, where the agglomerates reduced free volume and decreased both tensile strength and elongation at break.

Dynamic mechanical analysis was conducted to examine the viscoelastic behavior of ZB-reinforced epoxy matrix composites. Figure 10(a)–(b) shows the storage (E') and loss (E'') modulus curves of the composite and pristine samples calculated as a function of temperature between 40°C and 140°C. In addition, the storage and loss modulus values for specific temperatures are given in Table 3. According to the results obtained, ZB additive showed significant effects on the storage modulus and loss modulus of the polymer composite. The storage modulus results showed a significant increase with ZB additive compared to the pristine sample. At 40°C, the storage modulus values for ZB1, ZB2, ZB3 and ZB4 samples increased by 66.4%, 66.7%, 52.1% and 61.1%, respectively, compared to the pristine sample. The loss modulus results showed the effect of ZB additive on the glass transition temperature (Tg) of the material more clearly. The insignificant peak in the pristine sample corresponds to a temperature of approximately 61°C, while the significant peaks for samples ZB1, ZB2, ZB3 and ZB4 correspond to a temperature of 65°C, 66°C, 64.5°C and 65.5°C, respectively. These peaks represent the glass transition temperature of the sample (Liu *et al.*, 2017).

Figure 9 Stress-strain curves of (a) ZB1, (b) ZB2, (c) ZB3 and (d) ZB4 samples after three-point bending test

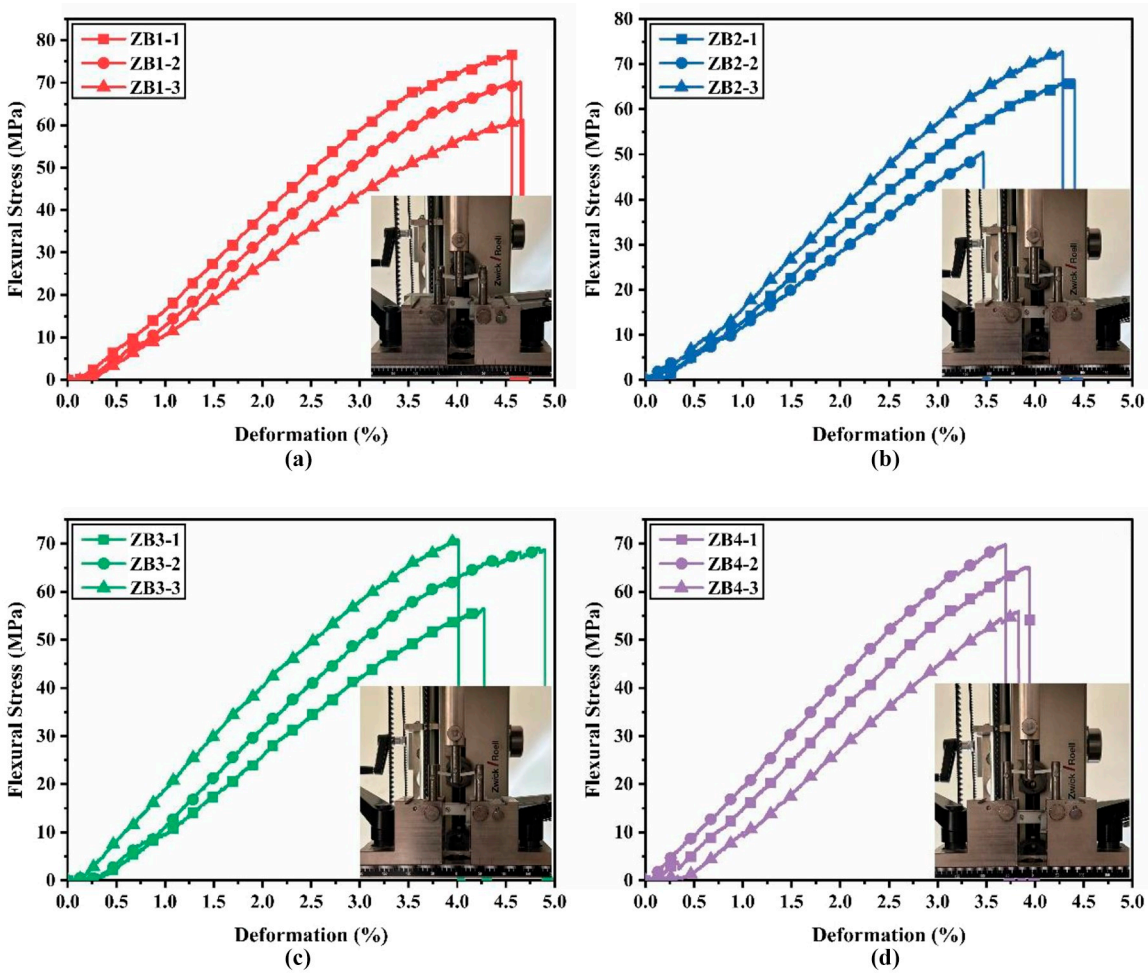

Source: Created by the authors

Figure 10 Storage (a) and loss (b) modulus curves as a function of temperature of pristine and ZB-reinforced composites

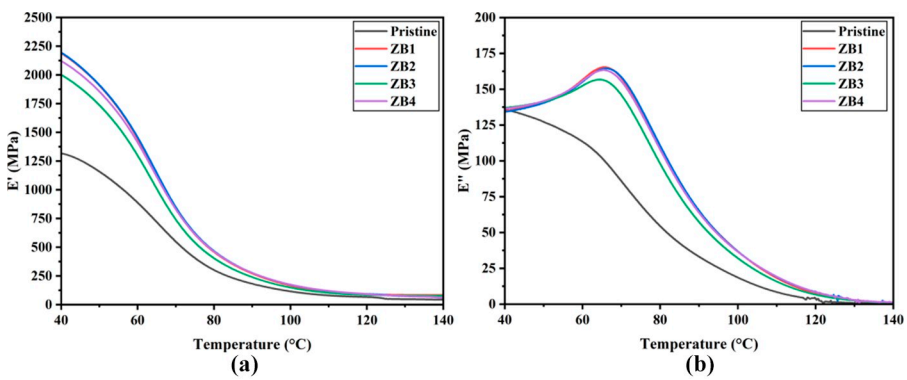

Source: Created by the authors

The observed increase in the Tg values of the samples with the ZB additive, the increase in their storage modulus and the preservation of this difference between the storage modulus values with increasing temperature indicate that composite materials that will operate at relatively high temperatures can perform better under dynamic loads and absorbing higher energy.

Figure 11 illustrates the impact of ZB) incorporation on the hardness (Shore D) of an epoxy acrylate-based resin using an SLA 3D printer. The data indicate a progressive increase in hardness with the addition of ZB in comparison to the pristine sample. The addition of ZB commences with 0.5 Wt.% (ZB1) and results in a notable increase in hardness, reaching the

Table 3 Storage modulus values of pristine and ZB-reinforced composites at different temperatures

E′ (MPa)	40°C	60°C	80°C	100°C	120°C
Pristine	1317.79	887.33	301.68	116.19	66.53
ZB1	2192.62	1446.14	456.12	166.46	90.95
ZB2	2196.14	1451.61	465.57	174.11	93.47
ZB3	2004.06	1297.85	404.85	150.08	84.92
ZB4	2122.44	1408.23	465.39	176.86	92.63

Source(s): Created by the authors

Figure 11 Shore D hardness values of pristine and ZB-reinforced composites

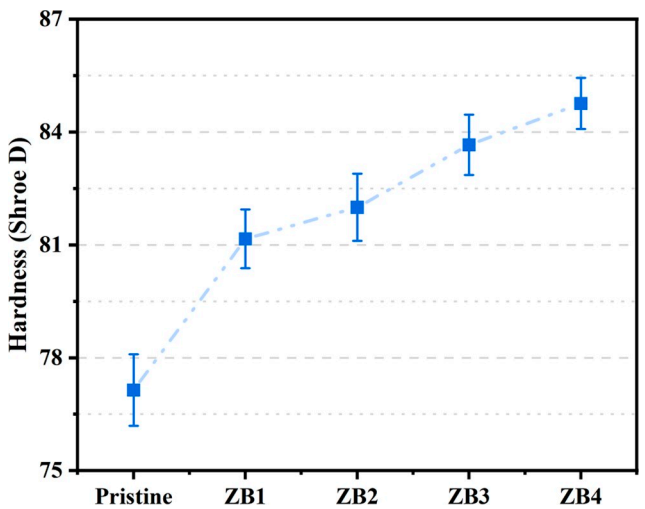

Source: Created by the authors

highest value of approximately 85 Shore D with 3 Wt.% (ZB4) of ZB.

The initial hardness of the pristine resin sample is approximately 80 Shore D. With the 0.5 Wt.% addition of ZB, the hardness increases to approximately 82 Shore D, and this trend continues as the amount of ZB is increased. These findings indicate that ZB markedly enhances the mechanical hardness of the resin, rendering it more suitable for applications that necessitate higher mechanical strength. It should be noted, however, that enhanced hardness does not inherently imply an improvement in overall mechanical strength. While hardness reflects the surface resistance to localized deformation, tensile and flexural properties are influenced by other factors such as the dispersion of the filler, interfacial adhesion and the ability of the matrix to transfer stress. Therefore, despite the increase in hardness with higher ZB content, this does not necessarily correlate with proportional improvements in tensile or bending strength, as discussed in previous sections.

These findings are consistent with previous studies in literature, which have demonstrated that the incorporation of ZB into various polymer composites can enhance mechanical properties. In addition, it has been reported that ZB not only improves hardness but also provides flame retardant properties in polymer matrices.

4. Conclusion

The findings of the study demonstrate that ZB plays a significant role in enhancing thermal and mechanical properties of composite structures. The ZB hydrate structure, as confirmed by XRD and FT-IR analyses, was found to enhance thermal stability by releasing gases that inhibit flame propagation while undergoing decomposition at elevated temperatures, as evidenced by TGA.

Furthermore, the mechanical properties are also markedly enhanced with the addition of ZB. The greatest increase was observed in the tensile test, with a 31.4% improvement, and in the three-point bending test, with a 39% improvement, in the sample (ZB1) with a 0.5% ZB addition by weight. These results are also consistent with the dynamic mechanical analysis, which indicates that agglomeration occurred with increasing additions, though this increase subsequently decreased. The ZB1 sample exhibited the most pronounced enhancements in both thermal stability and mechanical properties. In the hardness analysis, it was observed that the hardness values also increased with increasing addition. This finding demonstrates the effectiveness of ZB addition in enhancing both mechanical properties and thermal stability.

The thermal conductivity test revealed a general increase in results, although there was a fluctuation in the data obtained with increasing rates. A review of the literature revealed that this phenomenon can be attributed to the restriction of phonon movement, which is responsible for thermal conductivity in agglomerates. The flammability test demonstrated that the rates used in the study were inadequate for enhancing flame retardancy, due to the insufficient quantity of particles on the sample surface.

Overall, this study validates the efficiency of ZB as an additive in industrial applications necessitating thermal resistance, offering environmental and economic benefits through the optimization of thermal performance in materials.

References

Burger, N., Laachachi, A., Ferriol, M., Lutz, M., Toniazzo, V. and Ruch, D. (2016), "Review of thermal conductivity in composites: mechanisms, parameters and theory", *Progress in Polymer Science*, Vol. 61, pp. 1-28, doi: 10.1016/j.progpolymsci.2016.05.001.

Canıtez, H., Yüksel Yılmaz, A.N. and Çelik Bedeloğlu, A. (2023), "The effect of silicon dioxide and zinc borate on the flame retardancy, thermal and mechanical properties of jute/epoxy hybrid composite", *Journal of Natural Fibers*, Vol. 20 No. 1, doi: 10.1080/15440478.2022.2131683.

Chan-Hom, T., Yamsaengsung, W., Prapagdee, B., Markpin, T. and Sombatsompop, N. (2017), "Flame retardancy, antifungal efficacies, and physical–mechanical properties for wood/polymer composites containing zinc borate", *Fire and Materials*, Vol. 41 No. 6, pp. 675-687, doi: 10.1002/fam.2408.

Cuthbertson, A.A., Lincoln, C., Miscall, J., Stanley, L.M., Maurya, A.K., Asundi, A.S., Tassone, C.J., Rorrer, N.A. and Beckham, G.T. (2024), "Characterization of polymer properties and identification of additives in commercially

available research plastics", *Green Chemistry*, Vol. 26 No. 12, pp. 7067-7090, doi: 10.1039/d4gc00659c.

Desai, S., Kamble, V., Ozarkar, V., Dingre, P., Desai, P., More, A., Mahajan, U., and Mhaske, S. (2024), "Designing of layered double hydroxide, metal oxides, and borate-reinforced thermoplastic polyurethanes composites", *Polymers for Advanced Technologies*, Vol. 35 No. 3, pp. 1-14, doi: 10.1002/pat.6334.

Dogan, M., Dogan, S.D., Savas, L.A., Ozcelik, G. and Tayfun, U. (2021), "Flame retardant effect of boron compounds in polymeric materials", *Composites Part B: Engineering*, Vol. 222, doi: 10.1016/j.compositesb.2021.109088.

Durrani, H., Sharma, V., Bamboria, D., Shukla, A., Basak, S. and Ali, W. (2020), "Exploration of flame retardant efficacy of cellulosic fabric using in-situ synthesized zinc borate particles", *Cellulose*, Vol. 27 No. 15, pp. 9061-9073, doi: 10.1007/s10570-020-03383-4.

Garcia, V.J., Cheng, X., Rong, L., Lara-Ceniceros, T.E., Ricohermoso, E., III, Bonilla-Cruz, J., Espiritu, R.D. and Advincula, R.C. (2024), "Thermomechanical properties of stereolithographic 3D-printed zinc oxide nanocomposites", *MRS Communications*, Vol. 14 No. 4, pp. 676-685, doi: 10.1557/s43579-024-00602-y.

Gillani, Q.F., Ahmad, F., Melor, P.S., Mutlib, M.I.A. and Ullah, S. (2018), "A synergy study of zinc borate in halloysite nanotube reinforced, siloxane epoxy base intumescent fire resistive coatings", *Materialwissenschaft Und Werkstofftechnik*, Vol. 49 No. 4, pp. 420-426, doi: 10.1002/mawe.201700254.

Guler, S., Yarali Cevik, Z.B., Firat, U., Demirgunes, S.B. and Ozler, B. (2025), "Investigation of titanium-reinforced polymer matrix nanocomposites fabricated by stereolithography for mechanical properties and activity in L929 cells", *Rapid Prototyping Journal*, Vol. 31 No. 9, pp. 1965-1976, doi: 10.1108/RPJ-09-2024-0410.

Gupta, R., Singh, M.K., Rangappa, S.M., Siengchin, S., Dhakal, H.N. and Zafar, S. (2024), "Recent progress in additive inorganic flame retardants polymer composites: Degradation mechanisms, modeling and applications", *Heliyon*, Vol. 10 No. 21, p. e39662, doi: 10.1016/j.heliyon.2024.e39662.

Liu, J., Sun, Y., Wang, W. and Chen, J. (2017), "Using the viscoelastic parameters to estimate the glass transition temperature of asphalt binders", *Construction and Building Materials*, Vol. 153, pp. 908-917, doi: 10.1016/j.conbuildmat.2017.07.120.

Lodha, S., Song, B., Park, S.I., Choi, H.J., Lee, S.W., Park, H.W. and Choi, S.K. (2023), "Sustainable 3D printing with recycled materials: a review", *Journal of Mechanical Science and Technology*, Vol. 37 No. 11, pp. 5481-5507, doi: 10.1007/s12206-023-1001-9.

Lu, N., Zhang, P., Wu, Y., Zhu, D. and Pan, Z. (2019), "Effects of size of zinc borate on the flame retardant properties of intumescent coatings", *International Journal of Polymer Science*, Vol. 2019, doi: 10.1155/2019/2424531.

Lv, Y.F., Thomas, W., Chalk, R. and Singamneni, S. (2020), "Flame retardant polymeric materials for additive manufacturing", *Materials Today: Proceedings*, Vol. 33, pp. 5720-5724, doi: 10.1016/j.matpr.2020.05.081.

Lv, Y., Dejus, D., Kobenko, S., Singamneni, S. and Glaskova-Kuzmina, T. (2022), "Evaluation of the fire-retardancy of ULTEM 9085 polymer composites processed by fused deposition modelling", *Materials Science*, Vol. 28 No. 3, pp. 353-359, doi: 10.5755/j02.ms.29976.

Mahajan, D.S., Deshpande, T.D., Bari, M.L., Patil, U.D. and Narkhede, J.S. (2020), "Hydrated and anhydrous zinc borate fillers for tuning the flame retardancy of epoxy nanocomposites", *Journal of Applied Polymer Science*, Vol. 137 No. 34, doi: 10.1002/app.48987.

Mubarak, S., Dhamodharan, D., B. Kale, M., Divakaran, N., Senthil, T., P., S., Wu, L. and Wang, J. (2020), "A novel approach to enhance mechanical and thermal properties of SLA 3D printed structure by incorporation of metal–metal oxide nanoparticles", *Nanomaterials*, Vol. 10 No. 2, p. 217, doi: 10.3390/nano10020217.

Muhammad, A., Rahman, M.R., Baini, R. and Bin Bakri, M.K. (2020), "Applications of sustainable polymer composites in automobile and aerospace industry", *Advances in Sustainable Polymer Composites*, pp. 185-207, doi: 10.1016/B978-0-12-820338-5.00008-4.

Ozcelik, G., Elcin, O., Guney, S., Erdem, A., Hacioglu, F. and Dogan, M. (2022), "Flame-retardant features of various boron compounds in thermoplastic polyurethane and performance comparison with aluminum trihydroxide and magnesium hydroxide", *Fire and Materials*, Vol. 46 No. 7, pp. 1020-1033, doi: 10.1002/fam.3050.

Peloquin, J., Kirillova, A., Rudin, C., Brinson, L.C. and Gall, K. (2023), "Prediction of tensile performance for 3D printed photopolymer gyroid lattices using structural porosity, base material properties, and machine learning", *Materials & Design*, Vol. 232, doi: 10.1016/j.matdes.2023.112126.

Perin, M., Quagliato, L., Berti, G.A., Jang, C., Jang, S. and Lee, T. (2023), "Manufacturing process, tensile-compressive, and impact properties of tungsten (W)-particle-reinforced SLA methacrylate", *Polymers*, Vol. 15 No. 24, p. 4728, doi: 10.3390/polym15244728.

Pinto, U.A., Visconte, L.L.Y. and Reis Nunes, R.C. (2001), "Mechanical properties of thermoplastic polyurethane elastomers with mica and aluminum trihydrate", *European Polymer Journal*, Vol. 37 No. 9, pp. 1935-1937, doi: 10.1016/S0014-3057(01)00069-6.

Raslan, H.A., Elnaggar, M.Y. and Fathy, E.S. (2019), "Flame-retardancy and physico-thermomechanical properties of irradiated ethylene propylene diene monomer inorganic composites", *Journal of Vinyl and Additive Technology*, Vol. 25 No. 1, pp. 59-67, doi: 10.1002/vnl.21615.

Russo, P., Acierno, D., Marletta, G. and Destri, G.L. (2013), "Tensile properties, thermal and morphological analysis of thermoplastic polyurethane films reinforced with multiwalled carbon nanotubes", *European Polymer Journal*, Vol. 49 No. 10, pp. 3155-3164, doi: 10.1016/j.eurpolymj.2013.07.021.

Sano, Y., Matsuzaki, R., Ueda, M., Todoroki, A. and Hirano, Y. (2018), "3D printing of discontinuous and continuous fibre composites using stereolithography", *Additive Manufacturing*, Vol. 24, pp. 521-527, doi: 10.1016/j.addma.2018.10.033.

Shan, W., Chen, Y., Hu, M., Qin, S. and Liu, P. (2020), "4D printing of shape memory polymer via liquid crystal display (LCD) stereolithographic 3D printing", *Materials Research*

Express, Vol. 7 No. 10, p. 105305, doi: 10.1088/2053-1591/abbd05.

Shen, K.K., Kochesfahani, S. and Jouffret, F. (2008), "Zinc borates as multifunctional polymer additives", *Polymers for Advanced Technologies*, Vol. 19 No. 6, pp. 469-474, doi: 10.1002/pat.1119.

Spieß, B., Metzsch-Zilligen, E. and Pfaendner, R. (2021), "Mechanistic evaluation of flame retardants during UL94 standard testing via IR-camera", *Polymer Testing*, Vol. 103, p. 107320, doi: 10.1016/j.polymertesting.2021.107320.

Tan, V.T., The Vinh, L., Tu Quynh, L., Thu Suong, H. and Dang Chinh, H. (2020), "A novel synthesis of nanoflower-like zinc borate from zinc oxide at room temperature", *Materials Research Express*, Vol. 7 No. 1, p. 015059, doi: 10.1088/2053-1591/ab67fa.

Tavangarian, F., Sadeghzade, S., Fani, N., Khezrimotlagh, D. and Davami, K. (2024), "3D-printed bioinspired spicules: strengthening and toughening via stereolithography", *Journal of the Mechanical Behavior of Biomedical Materials*, Vol. 155, p. 106555, doi: 10.1016/j.jmbbm.2024.106555.

Tugrul, N., Bardakci, M. and Ozturk, E. (2015), "Synthesis of hydrophobic nanostructured zinc borate from zinc carbonate, and characterization of the product", *Research on Chemical Intermediates*, Vol. 41 No. 7, pp. 4395-4403, doi: 10.1007/s11164-014-1538-4.

Tuli, N.T., Khatun, S. and Rashid, A.B. (2024), "Unlocking the future of precision manufacturing: a comprehensive exploration of 3D printing with fiber-reinforced composites in aerospace, automotive, medical, and consumer industries", *Heliyon*, Vol. 10 No. 5, doi: 10.1016/j.heliyon.2024.e27328.

Yildiz, B., Seydibeyoğlu, M.Ö. and Güner, F.S. (2009), "Polyurethane-zinc borate composites with high oxidative stability and flame retardancy", *Polymer Degradation and Stability*, Vol. 94 No. 7, pp. 1072-1075, doi: 10.1016/j.polymdegradstab.2009.04.006.

Yücesoy, A., Balçik Tamer, Y. and Berber, H. (2023), "Improvement of flame retardancy and thermal stability of highly loaded low density polyethylene/magnesium hydroxide composites", *Journal of Applied Polymer Science*, Vol. 140 No. 30, pp. 1-17, doi: 10.1002/app.54107.

Zhou, D., Luo, Q., Nie, G., Dong, M., Du, X., Liu, H., Wu, Z. and Li, J. (2024a), "Preparation of high-quality zinc borate flame retardant: the existence mechanism and synergistic coupling separation of chloride ions in zinc borate", *Separation and Purification Technology*, Vol. 344, doi: 10.1016/j.seppur.2024.127198.

Zhou, X., Huang, X., Zhang, L., Zheng, L., Wang, R., Wu, L. and Weng, Z. (2024b), "Preparation of high thermal conductivity vat photopolymerization used UV-curable resin synergistically enhanced by silicon nitride and boron nitride", *Ceramics International*, Vol. 50 No. 13, pp. 23441-23450, doi: 10.1016/j.ceramint.2024.04.066.

Further reading

Feng, C., Zhang, Y., Liang, D., Liu, S., Chi, Z. and Xu, J. (2015), "Influence of zinc borate on the flame retardancy and thermal stability of intumescent flame retardant polypropylene composites", *Journal of Analytical and Applied Pyrolysis*, Vol. 115, pp. 224-232, doi: 10.1016/j.jaap.2015.07.019.

Corresponding author

Saadet Guler can be contacted at: saadet.guler@ikcu.edu.tr